



The pathogenic AGT c.856+1G>T mutation of a patient with multiple renal cysts and hypertension

Wenqing Chen^{1,2,3,4,5#}, Bingjue Li^{1,2,3,4,5#}, Sha Jia^{1,2,3,4,5}, Qixia Shen^{1,2,3,4,5}, Chong Luo^{1,2,3,4,5}, Yucheng Wang^{1,2,3,4,5}, Shi Feng^{1,2,3,4,5}, Xiujin Shen^{1,2,3,4,5}, Chunhua Weng^{1,2,3,4,5}, Hong Jiang^{1,2,3,4,5}, Jianghua Chen^{1,2,3,4,5}

¹Kidney Disease Center, the First Affiliated Hospital, College of Medicine, Zhejiang University, Hangzhou 310003, China; ²Key Laboratory of Nephropathy, Zhejiang Province, Hangzhou 310000, China; ³Kidney Disease Immunology Laboratory, the Third-Grade Laboratory, State Administration of Traditional Chinese Medicine of China, Hangzhou 310000, China; ⁴Key Laboratory of Multiple Organ Transplantation, Ministry of Health of China, Hangzhou 310000, China; ⁵Institute of Nephropathy, Zhejiang University, Hangzhou 310003, China

#These authors contributed equally to this work.

Correspondence to: Prof. Jianghua Chen; Prof. Hong Jiang. Kidney Disease Center, the First Affiliated Hospital, College of Medicine, Zhejiang University, Qingchun Road 79, Hangzhou 310003, China. Email: chenjianghua@zju.edu.cn; jianghong961106@zju.edu.cn.

Abstract: Angiotensinogen (AGT) is an essential member of the renin-angiotensin system (RAS); this system regulates blood pressure and affects the physiological function of the kidney. Studies found that mutations of the human AGT gene are involved in diseases such as recessive renal tubular dysgenesis (RTD) and essential hypertension (EHT). Here, we report a 29-year-old male Chinese with essential hypertension and cystic kidney disease. Exome sequencing analysis of the patient and his parents revealed a mutation in the splice donor site of intron 2 of the AGT gene, c.856+1G>T. This mutation was a heterozygous form and inherited from his mother, and the mother was diagnosed with essential hypertension lasting over 20 years. Function prediction of c.856+1G>T mutation using online software showed this intron mutation may affect protein features by destroying the normal splice site. These findings suggest that this intron mutation of the AGT gene is related to the patient's essential hypertension and cystic kidney disease.

Keywords: Renal cyst; AGT gene; intron mutation; hypertension

Submitted Jul 06, 2019. Accepted for publication Sep 30, 2019.

doi: 10.21037/atm.2019.10.64

View this article at: <http://dx.doi.org/10.21037/atm.2019.10.64>

Introduction

Angiotensinogen (AGT) is the precursor of angiotensin peptides in the renin-angiotensin system (RAS) (1). The RAS plays a key role in regulating blood pressure and physiological function of the kidney. The human *AGT* gene is located on chromosome 1q42 and composed of 5 exons (4 coding exons) (1). Several mutations of *AGT* gene (rs74315283; rs121912702; rs387906578) have been reported to cause a severe fetal disorder autosomal recessive renal tubular dysgenesis (RTD; OMIM 267430) (2,3). Also, the *AGT* gene was associated with essential hypertension (EHT; OMIM 145500) in many studies.

EHT is the most common type of hypertension, accounting for almost 95% of all hypertensive cases. EHT is a heterogeneous disease of which the exact pathogenesis is still

unknown. At present, people think this disorder is caused by interactions between the environment and genetic factors (4). In the past few years, with the development of genetic testing technologies, people have paid more attention to genetic factors of hypertension. The genetic linkage between the *AGT* gene and EHT has been widely studied in the past few decades (5). Case-control studies and systematic reviews from different races have shown that several variants of the *AGT* gene are more common in EHT patients (6,7).

Cystic kidney disease is another heterogeneous disease characterized by the formation of fluid-filled sacs in the kidneys (8). This disorder is a key cause of chronic end-stage renal disease (ESRD) (9). Among this complex disorder, several types have been confirmed to be hereditary cystic kidney diseases, such as autosomal recessive

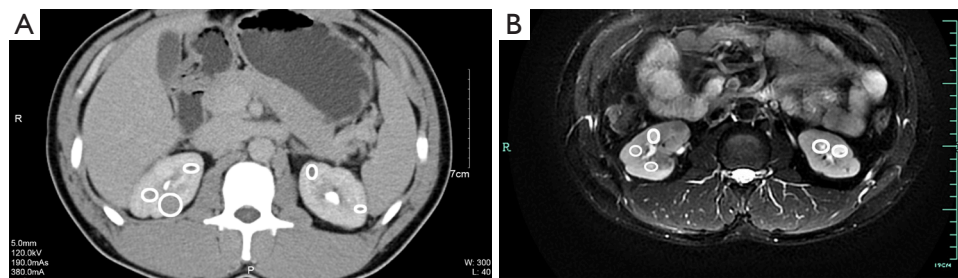


Figure 1 Typical renal cystic structures of the patient's kidneys. (A) Typical renal cystic structures of the enhanced CT image of the patient's kidneys. (B) Typical renal cystic structures of the magnetic resonance imaging of the patient's kidneys. White circles mark the cystic structures.

polycystic kidney disease (ARPKD), nephronophthisis, and Bardet-Biedl syndrome (10). Abnormal expression of angiotensinogen was found to be associated with the formation of cysts in ARPKD mouse model (11).

Tabei *et al.* conducted a case-control study and found that the allele frequency of *AGT-TT* genotype (M235T) differed significantly from patients with both hypertension and simple renal cysts and normal individuals (12). This means the *AGT* gene may be involved in both hypertension and renal cyst formation. Here, we present a case of an intron mutation of the *AGT* gene in a patient with both hypertension and multiple renal cysts.

Case presentation

Clinical history and laboratory data

The patient was a 29-year-old male Chinese, and a mildly elevated serum creatinine level was found on laboratory evaluation beginning in 2010 because of his lower back pain caused by urolithiasis. One week later, the patient's serum creatinine returned to 130 $\mu\text{mol/L}$ (normal range 44–133 $\mu\text{mol/L}$) and urine protein was negative in the local hospital. Ultrasonography displayed multiple cystic structures of both kidneys, a hamartoma, and several calculi in the right kidney. His serum creatinine remained at 130–160 $\mu\text{mol/L}$ over the next few years, and urine protein levels were maintained between “trace” and “1+”. Also, elevated blood pressure was found in his first hospitalization; however, detailed blood pressure level data were unavailable.

In 2014, the patient's other ultrasonography showed a hypoechoic nodule and multiple echogenic nodules in his right kidney, and multiple cystic structures in both kidneys. Two months later, in 2015, he went to another hospital for aggravated lower abdominal distension. An enhanced helical

CT scan of the kidneys showed a clearer image of multiple kidney cysts: this patient had 11 cysts in the right kidney and 5 cysts in the left kidney (*Figure 1A*). He then accepted laparoscopic partial nephrectomy of the right kidney. The diagnostic report on pathologic tissues at urology surgery in 2015 indicated renal angioliomyoma of the right kidney (*Figure S1*). In this hospitalization, his serum creatinine levels swung between 140 and 165 $\mu\text{mol/L}$, urine protein was detected as “1+” several times, and the highest systolic blood pressure was 150 mmHg.

He was later referred to our nephrology outpatient clinic in 2017. Detailed examination showed a serum creatinine level of 166 $\mu\text{mol/L}$ (normal range 59–104 $\mu\text{mol/L}$), estimated glomerular filtration rate (eGFR) of 47.27 ml/min using the Chronic Kidney Disease-Epidemiology Collaboration (CKD-EPI) [based on serum creatinine] equation, and urine protein 0.7 g/L (normal range 0.010–0.140 g/L) (*Table 1*). Routine blood tests showed an erythrocytosis, and bone marrow cytology displayed active erythroid hyperplasia (*Table S1*). We tested for the JAK2 mutation (p.V617F) in the patient but found no such mutation. The result of magnetic resonance imaging (MRI) in kidneys showed that this patient had 8 cysts in the right kidney (postoperative) and 7 cysts in the left kidney (*Figure 1B*). On ultrasound, the kidneys were echogenic and borderline small, measuring 9.9 cm on the right and 8.8 cm on the left, and there were multiple cystic structures of various sizes in both kidneys, with the biggest being nearly 1.2 cm \times 1.5 cm in the right kidney. Multiple small stones were present in both kidneys, and multiple echogenic nodules were in the right kidney (hamartoma); however, no cysts were found in the liver (*Figure 2*). There were no abnormalities in his parents' kidneys or liver ultrasonography (*Figure S2*). Physical examination showed a blood pressure of 144/110 mm Hg. His mother was diagnosed with hypertension lasting for over 20 years.

Table 1 Clinical data of the patient and family members

Subject	Sex	Age [†] , yr.	Serum				eGFR, >90 mL/min	Genetic analysis of AGT gene				
			Bp, <130/90 mmHg	Glu, 3.90–6.10 mM	K, 3.5–5.2 mM	Cr, 45–84 μm (F) 59–104 μm (M)		Bun, 2.90–8.20 mM	Uric acid, 155–357 μm (F) 208–428 μm (M)	AGT, pg/mL	Nucleotide change	Function change
Patient	M	29	144/110	3.43	3.34	166	6.70	522	1,467.23	47.27	c.856+1G>T	Splicing
Mother	F	51	135/81	4.98	4.30	58	5.60	364	1,542.73	102.81	c.856+1G>T	Splicing
Father	M	56	129/87	5.12	4.54	77	5.91	389	2,452.64	96.46	–	–

Bp, blood pressure; Glu, glucose; K, potassium; Cr, creatinine; Bun, blood urea nitrogen; M, male; F, female. [†]Age at first examination at our hospital.

The patient's medical history included gout and renal hamartoma. Medications included allopurinol tablets 0.2 g and sodium bicarbonate 0.5 g daily for 2 years. Due to the ultrasonography changes in this patient's kidneys and continuous renal function impairment with hypertension, to identify simple renal cyst and polycystic kidney disease, we performed a gene test. The sequencing analysis of the patient and his parents revealed a heterozygous intron mutation in the *AGT* gene (c.856+1G>T), and no variants in *PKD1*, *PKD2*, or *PKHD1* were detected. *PKD1* gene has 7 pseudogenes that make its coverage in exome sequencing insufficient to exclude the presence of pathogenic variation. Thus, further experimentation applying long-PCR and Sanger sequencing to screen *PKD1* variations is underway. Apart from this, this patient had both renal hamartoma and renal cysts, so we needed to distinguish it from tuberous sclerosis. However, no variants in *TSC* genes were detected. We also performed immunohistochemical staining of *AGT* protein using paraffin sections of surgically removed tissue in 2015, but we could not detect kidney tissues under the microscope (data not shown). To verify whether this mutation can affect angiotensinogen protein expression, we used an enzyme-linked immunosorbent assay (ELISA) to measure the serum levels of angiotensinogen. Results showed that the patient and his mother had lower serum angiotensinogen levels than his father (*Table 1*). We tested the RAS system of the patient and his parents (*Table 2*). We found that the patient and his mother had significantly higher levels of angiotensin I-converting enzyme (ACE) and aldosterone than his father. The patient, in particular, had a significantly higher level of ACE than normal.

Diagnosis and treatments

Chronic kidney disease stage III, cystic kidney disease, and essential hypertension.

Clinical follow-up

Following the diagnosis, the patient accepted medications of losartan potassium 100 mg/corbrin 0.4 g daily for one week. At the time of patient discharge, the creatinine level improved slightly to 165 μmol/L (estimated GFR, 47.62 mL/min), blood pressure was 110/77 mmHg, and proteinuria decreased to 0.2 g/L. At his latest evaluation, 6 months after discharge, serum creatinine level was 185 μmol/L (estimated GFR, 41.17 mL/min) with proteinuria at 1.0 g/L and blood pressure at 123/83 mmHg.



Figure 2 Ultrasound image of the patient's kidneys and liver. (A) Left kidney. (B) Right kidney. (C) Liver. White circles mark the dark areas.

Table 2 The RAS system data of the patient and family members

Subject	Plasma		Serum		ARR
	Renin (4.4–46.1) mIU/L	Aldosterone (3.0–35.3) ng/L	AGT, pg/mL	ACE (24–139) U/L	
Patient	27.99	99.50	1,467.23	192	3.55
Mother	24.15	87.60	1,542.73	126	3.63
Father	18.23	33.20	2,452.64	52	1.82

ACE, angiotensin I-converting enzyme; ARR, aldosterone-to-renin ratio.

Mutation analysis of the AGT gene

The sequence analysis of the patient and his parents revealed a heterozygous intron mutation in the *AGT* gene (c.856+1G>T) (Supplemental File). The mutation was localized in an evolutionary conservation nucleotide (IVS856+1) of intron 2 (Figure 3A,B,C). Sequence analysis showed that the variant was inherited from his mother. Next, we performed Sanger sequencing in the proband and his parents for the validation of the *AGT* gene variant (Figure 3D). Forward *AGT* primer: CTGTGGATGAAAAGGCCCTA, reverse *AGT* primer: ACCCCAGTTCCTGACCTTCT.

Functional changes prediction of c.856+1G>T mutation

This splice variant destroys the established splice donor site, and the ClinVar database predicted this mutation might lead to an abnormal message or an abnormal protein product. Web-based software MutationTaster predicted this mutation was disease-causing, capable of causing splice site change and affecting protein features (Figure 4). Human splicing finder 3.1 (HSF 3.1) is a software to identify and predict mutations' effect on splicing motifs. The results of its algorithms indicated that the c.856+1G>T mutation may

break a normal donor splice site and create a new donor splice site (Figure 5). Also, SPIDEX index predicted the mutation could probably change splicing, while Combined Annotation Dependent Depletion (CADD) score predicted the mutation might be a pathogenic one (Table 3). Since mRNA of *AGT* gene was faintly expressed in peripheral blood and blood cells as demonstrated in another study (Figure S3) (13), we did not make a polymerase chain reaction to verify whether the mRNA was affected. The c.856+1G>T variant is not observed at a significant frequency in large population cohorts (14,15).

Discussion

AGT is the precursor of angiotensin peptides in the renin-angiotensin system (RAS), and plays a key role in regulating blood pressure and renal physiological function as an essential member of the RAS (1). The human *AGT* gene is located on chromosome 1q42 and is composed of 5 exons, and several pathogenic variants of the *AGT* gene have been observed. Among these deleterious allelic variants are those associated with susceptibility to essential hypertension (NM_000029.3: p.T242I, p.L244R, and p.Y281C) (6,7). With the popularization of gene test application in clinical

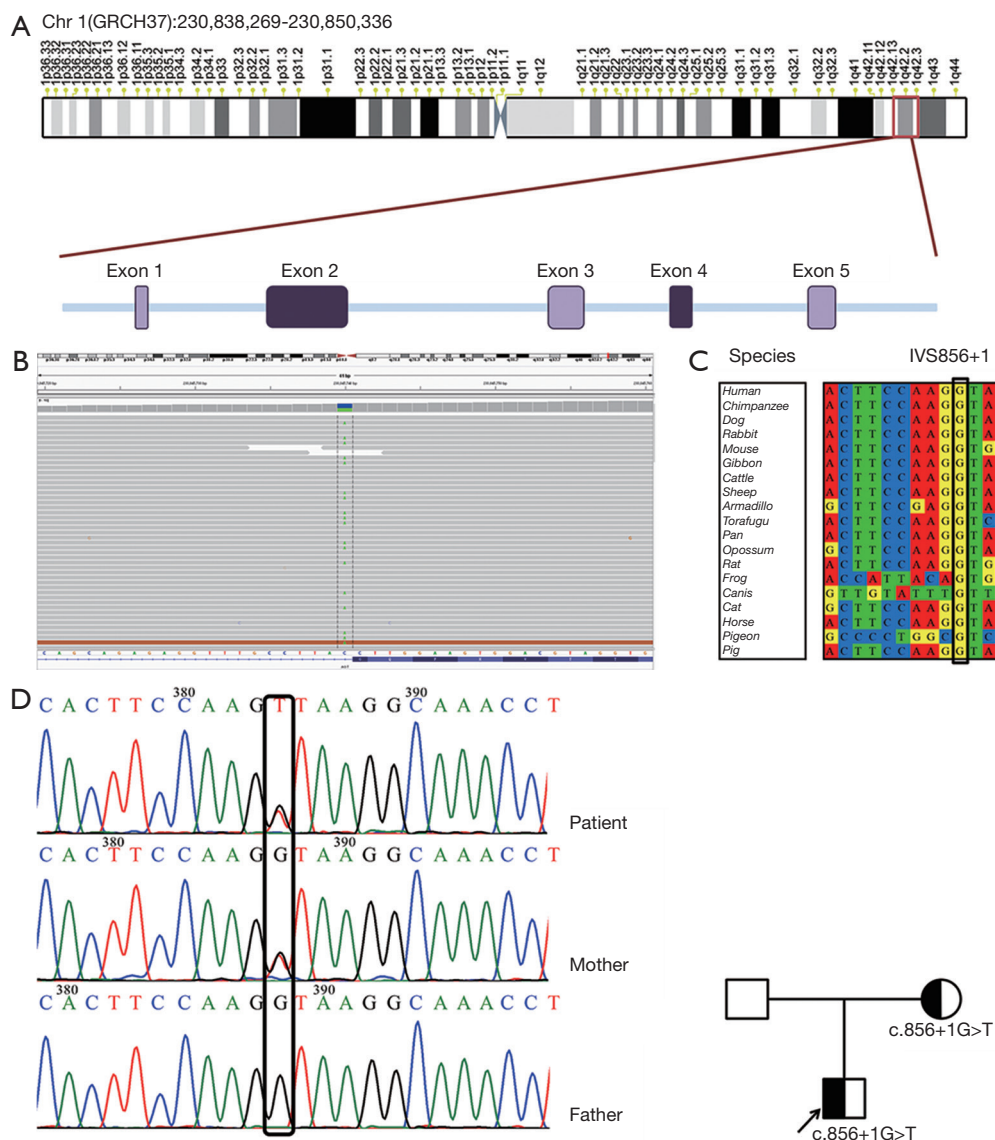


Figure 3 Sequencing analysis and evolutionary conservation of the *AGT* gene and the c.856+1G>T variant. (A) Genomic structure of the human *AGT* gene located at chromosome 1. (B) IGV schematic diagram of the *AGT* gene c.856+1G>T mutation site. The black dotted frame depicts the cDNA position of the mutation site. (C) Evolutionary conservation of IVS856+1 using the ClustalX program. The black frame marks the IVS856+1 site. (D) Chromatograms for the mutations confirmed by Sanger sequencing and pedigree of the family. Patient (up), mother (middle), father (down).

diagnosis and therapy, more *AGT* gene single-nucleotide polymorphisms have been detected, but most of them are non-pathogenic (16).

In this report, we found a previously reported intron mutation site of the *AGT* gene in a 29-year-old male Chinese with multiple renal cysts and hypertension. It is a heterozygous mutation inherited from the mother. The clinical symptoms of this patient were special; hypertension

and renal impairment were found at an early age but progressed slowly. His creatinine level has remained at 130–160 $\mu\text{mol/L}$ for many years, urine protein levels have been maintained between “trace” and “1+,” and medical imaging examination has displayed multiple cystic structures in both kidneys. The DNA sequencing analysis of the patient showed no mutation in polycystic kidney disease or tuberous sclerosis relative genes, so he was diagnosed with

Analyzed issue			Analysis result
Summary			-Protein features (potentially) affected -Splice site changes
Name of alteration			c.856+1G>T
HGNC symbol			AGT
Alteration location			Chr1:230845740C>A
Alteration type			Single base exchange
Alteration region			Intron
DNA changes			g.4304G>T
Splice sites			Alteration within used splice site, likely to disturb normal splicing
Protein features			Details
Start (aa)	End (aa)	feature	
277	288	STRAND	Might get lost (downstream of altered splice site)
291	293	STRAND	Might get lost (downstream of altered splice site)
302	305	STRAND	Might get lost (downstream of altered splice site)
304	394	CARBOHYD N-linked	Might get lost (downstream of altered splice site)
313	322	STRAND	Might get lost (downstream of altered splice site)
325	328	TURN	Might get lost (downstream of altered splice site)
328	328	CARBOHYD N-linked	Might get lost (downstream of altered splice site)
329	333	STRAND	Might get lost (downstream of altered splice site)
333	333	CONFLICT	Might get lost (downstream of altered splice site)
337	339	TURN	Might get lost (downstream of altered splice site)
340	349	STRAND	Might get lost (downstream of altered splice site)
353	358	HELIX	Might get lost (downstream of altered splice site)
365	368	HELIX	Might get lost (downstream of altered splice site)
374	381	STRAND	Might get lost (downstream of altered splice site)
385	391	STRAND	Might get lost (downstream of altered splice site)
392	395	HELIX	Might get lost (downstream of altered splice site)
402	406	HELIX	Might get lost (downstream of altered splice site)
407	409	STRAND	Might get lost (downstream of altered splice site)
425	434	STRAND	Might get lost (downstream of altered splice site)
452	455	STRAND	Might get lost (downstream of altered splice site)
460	466	STRAND	Might get lost (downstream of altered splice site)
467	470	TURN	Might get lost (downstream of altered splice site)
475	479	STRAND	Might get lost (downstream of altered splice site)

Figure 4 Evaluation of the pathogenic potential of c.856+1G>T mutation in the AGT gene using web-based software MutationTaster. Protein features showed the detailed predicted protein functional changes caused by the c.856+1G>T mutation.

cystic kidney disease.

Additionally, routine blood tests and bone marrow cytology suggested erythrocytosis in this patient, and no V617F mutation in the *JAK2* gene was detected, we excluded polycythemia vera and considered it a secondary erythrocytosis resulting from focal renal ischemia caused by renal cyst compression (17). Because of his slowly progressing renal impairment and the fact that there was no manifestation of hematuria, we considered that neither renal cell carcinoma nor hamartoma could cause these clinical symptoms. It is believed that the RAS is activated in polycystic kidney disease, and perhaps due to renal ischemia caused by cyst expansion (18). Tabei *et al.* completed a case-control study and found that the allele frequency of *AGT-TT* genotype (M235T) differed significantly between patients with both hypertension and simple renal cysts and

normal individuals (12). Animal experiments using *Pkd1* and *Pkd2* mice indicated that blockade angiotensinogen could attenuate cystogenesis (19,20). In summary, we thought the renal cysts might be the cause of renal function injury in this patient, and cystogenesis had a relationship with the c.856+1G>T mutation. Future studies are needed to elucidate the mechanisms through which this association is mediated.

The patient developed hypertension at an early age (nearly 20 years old), and his mother, carrying the same heterozygous mutation of *AGT* gene, also developed hypertension at a relatively early age (nearly 30 years old) compared with other hypertensive patients. We therefore speculated the c.856+1G>T mutation in *AGT* gene was also involved in their status of hypertension. On the other hand, we thought that the “two-hit” model proposed for cystogenesis in autosomal dominant polycystic kidney

Predicted signal	Prediction algorithm	cDNA Position		Interpretation							
New donor site	†HSF Matrices	T T C C A A G t t a a g g c a		-Activation of an intronic cryptic donor site -Potential alteration of splicing							
Broken WT donor site	†HSF Matrices †MaxEnt	T C C A A G g t a a g g c a a		-Alteration of the WT donor site, most probably affecting splicing							
Potential splice sites											
1.HSF matrices											
Sequence position	cDNA position	Splice site type	Motif	New splice site	Wild type	Mutant	If cryptic site use, exon length variation	Variation (%)			
845	845	Acceptor	TCCACTTCCAAGgt	tccactccaagTT	82.87	78.58	-845	-5.18			
850	850	Acceptor	TTCCAAGgtaaggc	ttccaagttaagGC	74.93	78.55	-850	+4.83			
853	853	Donor	CAAGgtaag	CAAgttaag	43.46	70.3	-853	New site +61.76			
854	854	Donor	AAGgtaagg	AAGttaagg	97.11	70.28	854	WT site broken -27.63			
2.MaxEnt											
Sequence position	cDNA Position	5' Motif					3' Motif				
		Ref Motif	Ref score	Mut motif	Mut score	Variation (%)	Ref motif	Ref score	Mut motif	Mut score	Variation (%)
837	837						CACCTACGTCCACTTCC AAGgta	4.97	cacctacgtccactccaag TTA	2.43	-51.11
854	854	AAGgta agg	10.51	AAGtta agg	2.01	-80.88					

Figure 5 Algorithms of predicting a mutation's effect on splicing motifs using HSF 3.1. †Consensus values go from 0 to 100 for HSF, -20 to +20 for MaxEnt. The threshold is defined at 65 for HSF, 3 for MaxEnt. If the WT score is above the threshold, and the score variation is under -10% for HSF (-30% for MaxEnt) this means the mutation breaks the splice site; if the WT score is under the threshold, and the score variation is above +10% for HSF (+30% for MaxEnt) this means the mutation creates a new splice site.

Table 3 Results of SPIDEX index and CADD score

Methods	Score
dPSI_percentile (SPIDEX)	0.05
CADD score	26.1

dPSI_percentile <3 in SPIDEX indicates the mutation may cause splicing changes. A higher score in CADD means a greater possibility of deleteriousness of a single nucleotide variant.

disease (ADPKD) could also explain the intra-familial phenotypic variability of multiple cystic structures being found on ultrasound in the patient's kidneys, but no abnormalities being found in his mother's kidneys (19,20). This hypothesis speculates that the cystogenesis in ADPKD includes two processes: the "first hit" is the germline mutation of an ADPKD gene, and the "second hit" refers to the somatic gene mutation affected by acquired factors such as infection. Here, the proband and his mother carried the same heterozygous mutation site of *AGT* gene; however, no cysts were detected in the mother's kidneys, which may be because she has not yet experienced the "second hit" stage.

To confirm the effect of this intron mutation on angiotensinogen protein expression, we tried to detect the cDNA fragments of different lengths of the *AGT* gene by PCR amplification and agarose gel electrophoresis using RNA isolated from peripheral blood cells; however, we failed to amplify the target *AGT* gene due to its low expression pattern in blood cells. Immunohistochemical staining of AGT protein was also performed using paraffin sections of surgically removed tissue of the patient in 2015. Regrettably, no kidney tissues were found under the microscope. ELISA measurement showed that the patient had a lower serum angiotensinogen level than his father (1,467.23 vs. 2,452.64 pg/mL), and that the serum angiotensinogen concentration of his mother was also lower than the father (1,542.73 vs. 2,452.64 pg/mL). We cannot conclude that the mutation is associated with plasma angiotensinogen level since the research sample size is too small. By testing the RAS system of the patient and his parents with the normal levels of plasma renin, we found that the patient and his mother had significantly higher levels of ACE and aldosterone than his father; the patient,

in particular, had a significantly higher level of ACE than normal.

Interestingly, with the further use of online software to predict the potential functional changes of this mutation site, various algorithms all indicated that the c.856+1G>T mutation in the *AGT* gene has the possibility of destroying the canonical splice donor site of intron 2 and affecting the features of the protein. MutationTaster, Human Splicing Finder 3.1, and SPIDEX made the same prediction that this mutation site may either leading to an abnormal message that is subject to nonsense-mediated mRNA decay, or to an abnormal protein product if the message is used for protein translation. After the literature search, we found this variant was not observed at a significant frequency in large population cohorts and has not been reported previously as a pathogenic variant nor as a benign variant.

In conclusion, we present a case of an intron mutation of the *AGT* gene in a 29-year-old male Chinese patient with multiple renal cysts and hypertension; it is a heterozygous mutation inherited from his mother. The patient's renal function impairment progressed slowly. His renal cystic lesion and hypertension seems to be due to the presence of a heterozygous c.856+1G>T mutation in the *AGT* gene. However, no direct experimental evidence proved that this mutation will affect angiotensinogen protein structure or function. Furthermore, we would like to confirm this notion in an animal model for hypertension in addition to performing a c.856+1G>T mutation of the *AGT* gene to see whether it affects renal cyst formation in a vitro cyst model.

Acknowledgments

We are grateful to all the staff at the Kidney Disease Center of the First Affiliated Hospital of Zhejiang University for their sincere support.

Funding: This work was supported by the National Natural Science Foundation of China (81770752 to J Chen, 81470938, 81770697 to H Jiang), and the Zhejiang Provincial Natural Science Foundation of China (LQ19H050004 to W Chen).

Footnote

Conflicts of Interest: The authors have no conflicts of interest to declare.

Ethical Statement: The research was conducted ethically in accordance with the World Medical Association Declaration of Helsinki. The study was approved by the Ethical

Committee of the Zhejiang University College of Medicine, the First Affiliated Hospital. The authors are accountable for all aspects of the work in ensuring that questions related to the accuracy or integrity of any part of the work are appropriately investigated and resolved. Written informed consent was obtained from the patient for publication of this manuscript and any accompanying images.

References

1. Fukamizu A, Takahashi S, Seo MS, et al. Structure and expression of the human angiotensinogen gene. Identification of a unique and highly active promoter. *J Biol Chem* 1990;265:7576-82.
2. Gribouval O, Gonzales M, Neuhaus T, et al. Mutations in genes in the renin-angiotensin system are associated with autosomal recessive renal tubular dysgenesis. *Nat Genet* 2005;37:964-8.
3. Uematsu M, Sakamoto O, Nishio T, et al. A case surviving for over a year of renal tubular dysgenesis with compound heterozygous angiotensinogen gene mutations. *Am J Med Genet A* 2006;140:2355-60.
4. Carretero OA, Oparil S. Essential hypertension. Part I: definition and etiology. *Circulation* 2000;101:329-35.
5. Jeunemaitre X, Soubrier F, Kotelevtsev YV, et al. Molecular basis of human hypertension: role of angiotensinogen. *Cell* 1992;71:169-80.
6. Li H, Du Z, Zhang L, et al. The relationship between angiotensinogen gene polymorphisms and essential hypertension in a Northern Han Chinese population. *Angiology* 2014;65:614-9.
7. Reiter LM, Christensen DL, Gjesing AP. Renin angiotensinogen system gene polymorphisms and essential hypertension among people of West African descent: a systematic review. *J Hum Hypertens* 2016;30:467-78.
8. Cramer MT, Guay-Woodford LM. Cystic kidney disease: a primer. *Adv Chronic Kidney Dis* 2015;22:297-305.
9. Chijioke A, Aderibigbe A, Olarenwaju TO, et al. Prevalence and pattern of cystic kidney diseases in Ilorin, Nigeria. *Saudi J Kidney Dis Transpl* 2010;21:1172-8.
10. König JC, Titieni A, Konrad M, et al. Network for Early Onset Cystic Kidney Diseases-A Comprehensive Multidisciplinary Approach to Hereditary Cystic Kidney Diseases in Childhood. *Front Pediatr* 2018;6:24.
11. Saigusa T, Dang Y, Mullick AE, et al. Suppressing angiotensinogen synthesis attenuates kidney cyst formation in a Pkd1 mouse model. *FASEB J* 2016;30:370-79.
12. Tabei SM, Nariman A, Daliri K, et al. Simple renal cysts

- and hypertension are associated with angiotensinogen (AGT) gene variant in Shiraz population (Iran). *J Renin Angiotensin Aldosterone Syst* 2015;16:409-14.
13. Su AI, Wiltshire T, Batalov S, et al. A gene atlas of the mouse and human protein-encoding transcriptomes. *Proc Natl Acad Sci U S A* 2004;101:6062-67.
 14. Lek M, Karczewski KJ, Minikel EV, et al. Analysis of protein-coding genetic variation in 60,706 humans. *Nature* 2016;536:285-91.
 15. 1000 Genomes Project Consortium, Auton A, Brooks LD, et al. A global reference for human genetic variation. *Nature* 2015;526:68-74.
 16. Amberger JS, Bocchini CA, Schiettecatte F, et al. OMIM.org: Online Mendelian Inheritance in Man (OMIM®), an online catalog of human genes and genetic disorders. *Nucleic Acids Res* 2015;43:D789-98.
 17. Stein BL, Oh ST, Berenzon D, et al. Polycythemia Vera: An Appraisal of the Biology and Management 10 Years After the Discovery of JAK2 V617F. *J Clin Oncol* 2015;33:3953-60.
 18. Chapman AB, Johnson A, Gabow PA, et al. The renin-angiotensin-aldosterone system and autosomal dominant polycystic kidney disease. *N Engl J Med* 1990;323:1091-6.
 19. Fitzgibbon WR, Dang Y, Bunni MA, et al. Attenuation of accelerated renal cystogenesis in Pkd1 mice by renin-angiotensin system blockade. *Am J Physiol Renal Physiol* 2018;314:F210-8.
 20. Ravichandran K, Ozkok A, Wang Q, et al. Antisense-mediated angiotensinogen inhibition slows polycystic kidney disease in mice with a targeted mutation in Pkd2. *Am J Physiol Renal Physiol* 2015;308:F349-57.

Cite this article as: Chen W, Li B, Jia S, Shen Q, Luo C, Wang Y, Feng S, Shen X, Weng C, Jiang H, Chen J. The pathogenic AGT c.856+1G>T mutation of a patient with multiple renal cysts and hypertension. *Ann Transl Med* 2019;7(22):699. doi: 10.21037/atm.2019.10.64

Materials and methods

Editorial policies and ethical considerations

All procedures performed in this study involving human participants were in accordance with the ethical standards of the research ethics committee of the First Affiliated Hospital of Zhejiang University and with the Helsinki declaration. This article does not contain any studies with animals performed by any of the authors. Informed consent was obtained from all individual participants included in the study.

DNA isolation and DNA quantification and qualification

Genomic DNA was extracted from 3 ml peripheral blood of the patient and his parents using Lab-Aid[®] 824 DNA Extraction Kit (Zeesan Biotech, Xiamen, China).

DNA purity was checked using the Nanodrop 2000[®] spectrophotometer (ThermoScientific, CA, USA). The DNA concentration was measured using the Qubit dsDNA HS Assay Kit on the Qubit[®] 3.0 Fluorometer (Life Technologies, CA, USA).

Library preparation for sequencing

A total amount of 1–3 µg DNA per sample was used as input material for the DNA sample preparations. Firstly, fragmentation was carried out using 1X Low TE Buffer (Life Technologies, CA, USA) in Covaris M220[®] ultrasonicator (Covaris, MA, USA) to obtain 150–200 bp DNA fragments. Subsequently, DNA fragments were purified with AMPure XP[®] system (Beckman Coulter, Beverly, MA, USA). Remaining overhangs were converted into blunt ends via DNA polymerase activities. After adenylation of 3' ends of DNA fragments, SureSelect Adaptor Oligo Mix (Agilent, CA, USA) were ligated to prepare for hybridization. PCR was then performed with HerculaSE II Fusion DNA Polymerase (Agilent, CA, USA), SureSelect Primer (Agilent, CA, USA), and SureSelect Reverse Prime (Agilent, CA, USA). Products were then purified with AMPure XP system, and concentration was measured on the Qubit[®] 3.0 fluorometer. At last, the library hybridization was performed in the SureSelect Hyb buffer system and captured in the SureSelect Library system; target enrichment and amplification, and barcode labeling were done following the manufacturer's recommendations.

Sequencing and analysis

The libraries were sequenced on an Illumina HiSeq 2500 (Illumina, San Diego, CA, USA) platform, and 75 bp paired-end reads were generated. Data analysis was made according to the Joingenome-ExomeSeq-V.1.1 (Joingenome Diagnosis, Hangzhou, China) analysis process. The cleaned reads were mapped to the human genome hg19 by BWA 0.7.12-R1039. SNPs were called out using GenomeAnalysisTK-3.3-0 and annotated with several public databases such as dbSNP (snp147), 1000 Genome (2015aug), ClinVar, ExAC, and OMIM. Online software including MutationTaster, CADD, and HSF 3.1 were used to predict the pathogenicity of the mutation.

ELISA analysis

To prepare samples for ELISA, 3 mL of whole blood per sample in VACUETTE[®] Z Serum Sep Clot Activator (Greiner Bio-One International, Frickenhausen, Germany) tubes were clotted for 1 h, and then centrifuged for 10 min at 1,000 g. Aspirate supernatant was aliquoted into small tubes and stored at –80 °C until use. Human Serpin A8/AGT DuoSet ELISA kit (R&D Systems, Minneapolis, MN, USA) was used to detect the serum AGT concentration. ELISA assays were performed according to protocols provided by the kit manufacturer.

Immunohistochemical analysis

Immunohistochemical analysis was performed on paraffin sections of surgically removed tissue of the patient in 2015; donor kidney tissue was used as normal control. To summarize, paraffin-embedded tissue slides were deparaffinized, rehydrated, and subjected to antigen unmasking by sodium citrate (pH 6.0) for 10 min at a sub-boiling temperature. Endogenous peroxidase activity was blocked by incubation in 0.3% hydrogen peroxide for 10 min. Sections were blocked with 5% BSA for 30 min at room temperature, followed by incubation with primary antibody overnight at 4 °C. For negative control, the anti-AGT antibody was replaced with 5% BSA. Sections were incubated with a horseradish peroxidase-conjugated secondary antibody for 30 min at room temperature. At last, sections were stained with the 3'-diaminobenzidine substrate and counterstained with hematoxylin, and dehydrated. Anti-AGT antibody was from NovusBio (cat: NBP1-30027SS, CA, USA).

The Second Affiliated Hospital Zhejiang University School of Medicine
Diagnostic report on pathologic tissues

Date when the sample was received: Jan.27, 2015

Report No: Surgical 2015-*****

Name of patient: *** Li	Pathologic Findings & Diagnosis Diagnostic conclusion: (Right kidney) Renal Angioleiomyoma Immunohistochemical results: vimentin ++, SMA ++, S-100 +, CD10 -, Melan-A +, HMB 45+, CK7 -, Ki-67 5-10%+, P53 -, CK(AE1/AE3) -.
Sex: Man Age: 28	
Name of department or ward: Urology Surgery	
Hospital bed No.: 5	
Outpatient or hospitalization No.: *****	
Tissue sent for examination: kidney	

Doctor: *** Wang

Report date: Feb.16, 2015

Figure S1 The diagnostic report on pathologic tissues at urology surgery of patient's right kidney.

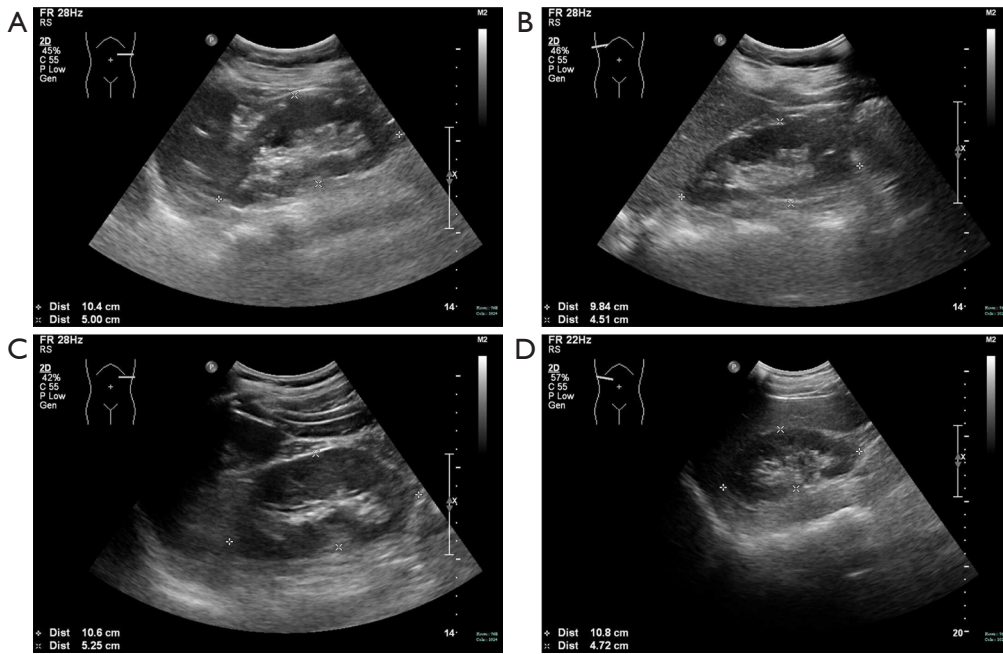


Figure S2 Ultrasound image of the parents' kidneys a. (A) The left kidney of the mother; (B) the right kidney of the mother; (C) the left kidney of the father; (D) the right kidney of the father.

GEO accession:	GSE1133
BioProject:	PRJNA87249
URL: https://www.ncbi.nlm.nih.gov/geo/query/acc.cgi?acc=GSE1133	
Samples	202834_at
721_B_lymphoblasts.	23.7
721_B_lymphoblasts.	23.6
Adipocyte.1	135.1
Adipocyte.2	141.2
AdrenalCortex.1	36.7
AdrenalCortex.2	38.8
Adrenalgland.1	57.8
Adrenalgland.2	49.8
Amygdala.1	734.7
Amygdala.2	1178.2
Appendix.1	32.3
Appendix.2	44.3
AtrioventricularNod	45.1
AtrioventricularNod	46.5
BDCA4+_DentriticCel	10.3
BDCA4+_DentriticCel	14.8
Bonemarrow.1	30.8
Bonemarrow.2	41.7
BronchialEpithelial	21.6
BronchialEpithelial	25.1
CD105+_Endothelial.	18.3
CD105+_Endothelial.	26.8
CD14+_Monocytes.1	8.9
CD14+_Monocytes.2	12.2
CD19+_BCells(neg._s	20
CD19+_BCells(neg._s	18.2
CD33+_Myeloid.1	24.4
CD33+_Myeloid.2	24.1
CD34+.1	25.4
CD34+.2	25.1
CD4+_Tcells.1	20
CD4+_Tcells.2	23.4

CD56+_NKCells.1	7.2
CD56+_NKCells.2	21.7
CD71+_EarlyErythroi	44.1
CD71+_EarlyErythroi	16.4
CD8+_Tcells.1	18.3
CD8+_Tcells.2	19.3
CardiacMyocytes.1	23.5
CardiacMyocytes.2	45.3
Caudatenucleus.1	597.4
Caudatenucleus.2	737.9
Cerebellum.1	497.4
Cerebellum.2	622.2
CerebellumPeduncles	780.8
CerebellumPeduncles	890
CiliaryGanglion.1	83
CiliaryGanglion.2	55.4
CingulateCortex.1	485.8
CingulateCortex.2	232
Colorectaladenocarc	25.1
Colorectaladenocarc	16
DorsalRootGanglion.	30.3
DorsalRootGanglion.	46.4
FetalThyroid.1	95.1
FetalThyroid.2	59.3
Fetalbrain.1	86.8
Fetalbrain.2	180.3
Fetalliver.1	4513.9
Fetalliver.2	3527.4
Fetallung.1	2312.1
Fetallung.2	3630.3
GlobusPallidus.1	164
GlobusPallidus.2	110.8
Heart.1	881.3
Heart.2	588.7
Hypothalamus.1	1074
Hypothalamus.2	1129.9

Kidney.1	220
Kidney.2	160.8
Leukemia_chronicMye	22.5
Leukemia_chronicMye	20.2
Leukemia_promyelocy	23.8
Leukemia_promyelocy	36.5
Leukemialymphoblast	14.5
Leukemialymphoblast	20.4
Liver.1	10504.2
Liver.2	6658
Lung.1	48
Lung.2	28.1
Lymphnode.1	21.6
Lymphnode.2	32.4
Lymphoma_burkitts(D	61.7
Lymphoma_burkitts(D	67.4
Lymphoma_burkitts(R	55.8
Lymphoma_burkitts(R	41.2
MedullaOblongata.1	284.3
MedullaOblongata.2	259.8
OccipitalLobe.1	386.4
OccipitalLobe.2	329.9
OlfactoryBulb.1	277
OlfactoryBulb.2	210.3
Ovary.1	19.4
Ovary.2	47.5
Pancreas.1	46.6
Pancreas.2	37.2
PancreaticIslet.1	106.3
PancreaticIslet.2	222.2
ParietalLobe.1	296.7
ParietalLobe.2	311
Pituitary.1	54.7
Pituitary.2	63.6
Placenta.1	19.5
Placenta.2	25.8

Pons.1	199.6
Pons.2	221.6
PrefrontalCortex.1	1212.7
PrefrontalCortex.2	1416.6
Prostate.1	54.4
Prostate.2	57.6
Salivarygland.1	34.5
Salivarygland.2	22.2
SkeletalMuscle.1	56.2
SkeletalMuscle.2	77.8
Skin.1	32.3
Skin.2	13.7
SmoothMuscle.1	26.9
SmoothMuscle.2	47.2
Spinalcord.1	3449.7
Spinalcord.2	2003.6
SubthalamicNucleus.	130.5
SubthalamicNucleus.	195.7
SuperiorCervicalGan	111.3
SuperiorCervicalGan	52.1
TemporalLobe.1	180.1
TemporalLobe.2	196.4
Testis.1	43.2
Testis.2	35
TestisGermCell.1	23.6
TestisGermCell.2	22.2
TestisInterstitial.1	20.6
TestisInterstitial.2	33.6
TestisLeydigCell.1	21.9
TestisLeydigCell.2	32.2
TestisSeminiferousT	56.7
TestisSeminiferousT	11.9
Thalamus.1	936
Thalamus.2	785.9
Thymus.1	24.1
Thymus.2	17.2

Thyroid.1	35.4
Thyroid.2	69.2
Tongue.1	50.5
Tongue.2	34.5
Tonsil.1	18.3
Tonsil.2	53.2
Trachea.1	44.5
Trachea.2	32.8
TrigeminalGanglion.	64.4
TrigeminalGanglion.	44.1
Uterus.1	13.1
Uterus.2	32.2
UterusCorpus.1	41.9
UterusCorpus.2	44.4
WholeBlood.1	17.4
WholeBlood.2	30
Wholebrain.1	731.3
Wholebrain.2	673.2
Colon.1	46.6
Colon.2	37.1
Pineal_day.1	66
Pineal_day.2	1131.1
Pineal_day.3	430.6
Pineal_day.4	135
Pineal_day.5	237.2
Pineal_night.1	256.4
Pineal_night.2	150.4
Pineal_night.3	63.3
Pineal_night.4	252.4
Pineal_night.5	172.1
Retina.1	1282.7
Retina.2	866.1
Retina.3	151.6
Retina.4	77.1
Small_intestine.1	51.6
Small_intestine.2	61.7

Figure S3 mRNA expression level of ATG in different tissues.

Table S1 Blood routine test results of patient during hospitalization and follow-up

Report time	Blood RBC count (4.09–5.74) $\times 10^{12}$ /L	Hb concentration 131–172 g/L	Hematocrit, Hct 38–50.8%
2017-05-15	6.33	195	58.2
2017-05-26	6.52	189	60.1
2017-05-27	6.86	195	62.9
2017-05-29	6.09	178	55.8
2018-02-01	6.80	206	52.7